

APPLICATION OF A NEURAL NETWORK FOR ESTIMATING THE CRACK FORMATION AND PROPAGATION IN SOL-GEL CeO₂ COATINGS DURING PROCESSING AT TEMPERATURE

UPORABA NEVRONSKE MREŽE ZA UGOTAVLJANJE NASTANKA IN ŠIRJENJA RAZPOKE V SOL-GEL PREMAZU CeO₂ MED POSTOPKOM OGREVANJA

Aydogan Savran¹, Musa Alcı¹, Serdar Yıldırım^{2,3}, Recep Yiğit^{3,4,5}, Erdal Çelik^{2,3,5}

¹Ege University, Dept. of Electrical and Electronics Engineering, 35100 Bornova, Izmir, Turkey

²Dokuz Eylül University, Dept. of Metallurgical and Materials Engineering, 35160 Buca, Izmir, Turkey

³Dokuz Eylül University, Center for Production and Applications of Electronic Materials (EMUM), 35160 Buca, Izmir, Turkey

⁴Dokuz Eylül University, Izmir Vocational School, Department of Technical Programs, 35150 Buca, Izmir, Turkey

⁵Dokuz Eylül University, Dept. of Nanoscience and Nanoengineering, 35160 Buca, Izmir, Turkey
recep.yigit@deu.edu.tr

Prejem rokopisa – received: 2012-09-21; sprejem za objavo – accepted for publication: 2013-10-28

In this study the application of a neural network to estimate the crack propagation and crack size in CeO₂ coatings on a Ni substrate during processing at temperature was evaluated as a function of the Ce content in solutions with increasing processing temperatures from 24 °C and 700 °C. In this respect, CeO₂ coatings were prepared on Ni tapes from solutions derived from Ce-based precursors using a sol-gel method for YBCO-coated conductors. The crack size of the coating was determined using an in-situ Hot-Stage ESEM depending on the temperature at a certain time in vacuum conditions. It was determined that the crack size of the coating increased with the increasing processing temperature. Measuring the crack sizes of the coatings using Hot-Stage ESEM is an expensive and time-consuming process. In order to eliminate these kinds of problems a neural-network approach was used to estimate the crack sizes of the coatings at different temperatures. The neural network was constructed directly from the experimental results. It was concluded that the estimation of the crack propagation of CeO₂ coatings on a Ni tape substrate are reasonable for the processing temperatures.

Keywords: CeO₂, sol-gel, neural network, crack

V tej študiji je bila ocenjena uporaba nevronske mreže za določanje širjenja razpoke in velikosti razpoke v premazu iz CeO₂ na podlagi iz Ni med ogrevanjem kot funkcija vsebnosti Ce v raztopini med ogrevanjem od 24 °C do 700 °C. Za ta namen je bil pripravljen premaz iz CeO₂ na traku iz Ni iz predhodne raztopine Ce z uporabo sol-gel metode za premaz na prevodniku YBCO. Velikost razpoke v premazu je bila določena v vročem z in-situ ESEM v odvisnosti od temperature po določenem času v vakuumu. Ugotovljeno je bilo, da velikost razpoke v premazu narašča z naraščanjem temperature procesa. Merjenje velikosti razpoke v vročem z uporabo ESEM je drag in časovno zamuden postopek. Za odpravo teh težav je bila za določanje velikosti razpoke v premazu pri različnih temperaturah uporabljena nevronska mreža. Ta je bila postavljena na podlagi eksperimentalnih rezultatov. Ugotovljeno je bilo, da je mogoče določanje širjenja razpoke v premazu CeO₂ na traku iz Ni pri različnih temperaturah procesa.

Ključne besede: CeO₂, sol-gel, nevronska mreža, razpoka

1 INTRODUCTION

Neural networks (NNs) possess massive parallelism, a powerful mapping capacity, and a learning property.¹ They are capable of making decisions based on incomplete, noisy and disordered information. In addition, they can provide reasonable outputs for inputs not encountered during training. Because of these properties they have gained the attention of scientist from many different areas. There are a huge number of papers in the area of control, identification and estimation.²⁻⁵ Most of the industrial productive processes exhibit a certain degree of nonlinearity. By means of their nonlinear mapping and learning properties, neural networks have been employed in the identification of unknown nonlinear systems.

The development of the new, high-temperature superconductors has resulted in many applications in the fields

of magnetic, electronic and microwave technologies. Ceramic superconductors have been deposited as thin films using various methods, e.g., electron-beam co-evaporation, chemical vapor deposition, ion-beam sputtering, pulsed-laser deposition and the sol-gel technique on many buffered substrates.⁶ CeO₂ is one of the buffer layers frequently used for surface-coated YBCO superconductors on textured nickel substrates.⁷ The sol-gel process offers a new possibility for the synthesis of oxide layers by applying liquid precursors to substrates by dipping, spinning or spraying methods.⁸ The major factors affecting the CeO₂ sol-gel coatings are the nature of the coating and the substrate, and the reaction parameters at the temperature of YBCO formation.⁹ The nature of the coatings are influenced by sol-gel parameters such as types of precursor, solvent and chelating agents, viscosity, Ce content, dilution, chelation, complexation, withdrawal rate, coating thickness and annealing conditions.

In particular, the cracks of buffer layers are the main problem in sol-gel processing.¹⁰

In our initial attempts¹¹ we determined the crack-propagation rate and the crack size of CeO₂ buffer layers on Ni tapes for YBCO-coated conductors using an in-situ, hot-stage, environmental scanning electron microscope (ESEM). In the present investigation, in order to determine the crack size of the CeO₂ sol-gel coatings by avoiding time-consuming and expensive experimental works, we propose to use a multilayer feed-forward NN to estimate the crack size at the processing temperatures.

2 NEURAL NETWORKS

Neural Networks (NNs) are massively parallel, distributed, adaptive, nonlinear information processing tools. They consist of simple nonlinear processing elements (PEs), referred to as neurons. Each neuron receives connections from other PEs and/or itself. The block diagram of a neuron is shown in **Figure 1**.

The neuron collects the values from all of its input connections, performs a predefined mathematical operation, and produces a single output value computed as:

$$y_j = f\left(\sum_{i=1}^n w_{ji}u_i + b_j\right) \quad (1)$$

where u_i is the input value, w_{ji} is the connection weight between the i^{th} input and the j^{th} neuron, and f is the activation function. The sum of the weighted inputs and the bias forms the input to an activation function f . The neurons may use any differentiable activation function f to generate their output. The sigmoid function is the one of the most common activation functions, as follows:

$$f(x) = \frac{1}{1 + e^{-x}} \quad (2)$$

The interconnectivity defines the topology of the NN. An important class of NNs is the multilayer feed-forward neural network, as shown in **Figure 2**. They consist of simple nonlinear processing elements (PEs) and weighted connections in a layered structure. The input signal propagates through the network in a forward direction from one layer to the next. The neurons are connected with weighted connections represented by the arrows in **Figure 2**.

The training of the NN is performed by adjusting the connection weights. It is performed by iteratively adjusting the weights (w) of the connections and biases (b) in the network in order to minimize a predefined cost function. A popular cost function is the sum of the squared error between the actual output and the desired output value for each unit in the output layer:

$$E = \frac{1}{2} \sum_k (t_k - y_k)^2 \quad (3)$$

where t_k is the desired or target response on the k^{th} unit and y_k is the produced network output on the same unit.

In order to perform training, a training set, including the input and desired response vectors, is prepared. The training is performed in two phases referred to as the forward and backward phases. In the forward phase, the input patterns from the training set are applied to the input layer. These inputs are multiplied by the associated weights, passed through the activation functions and transferred to the next layer. They propagate through the network, layer by layer. Finally, the actual response of the network is produced at the output layer. The errors between the desired and the network outputs are found. In the backward phase, the error signal propagates backwards through the network and the gradients are computed. These are then used to determine the weight changes in the net according to used learning rule. A more common learning algorithm is the back-propagation algorithm, which is introduced in¹².

The standard back-propagation implements the steepest-descent method (also called the gradient-descent method). At each step of the steepest-descent method the weights are adjusted in the direction in which the error function decreases most rapidly. This direction is determined by the gradient of the error surface at the current point in the weight space. The weights are updated in a negative direction to the gradient with a certain rate, as given by:

$$\begin{aligned} w_{ji}^{\text{new}} &= w_{ji}^{\text{old}} - \eta \frac{\partial E}{\partial w_{ji}} \\ w_{lj}^{\text{new}} &= w_{lj}^{\text{old}} - \eta \frac{\partial E}{\partial w_{lj}} \\ w_{kl}^{\text{new}} &= w_{kl}^{\text{old}} - \eta \frac{\partial E}{\partial w_{kl}} \end{aligned} \quad (4)$$

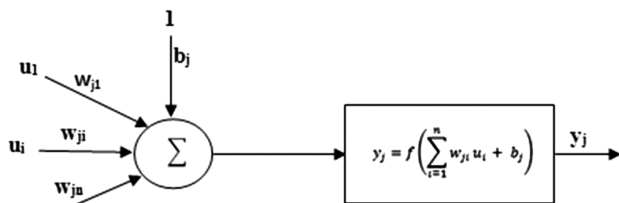


Figure 1: Artificial neuron model

Slika 1: Model umetne nevronske mreže

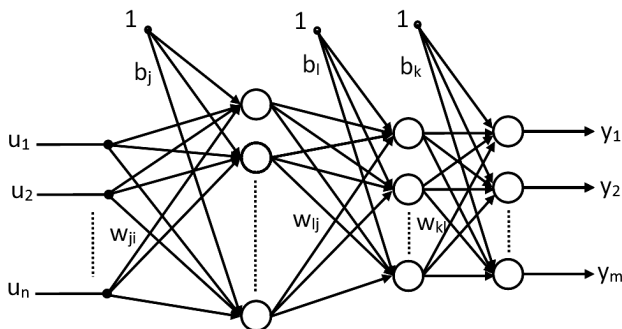


Figure 2: Multilayer feed-forward neural network

Slika 2: Večplastno napajanje nevronske mreže

in which η is the learning rate that determines the step size through the gradient direction. Similarly, the biases are updated as follows:

$$\begin{aligned} b_j^{\text{new}} &= b_j^{\text{old}} - \eta \frac{\partial E}{\partial b_j} \\ b_l^{\text{new}} &= b_l^{\text{old}} - \eta \frac{\partial E}{\partial b_l} \\ b_k^{\text{new}} &= b_k^{\text{old}} - \eta \frac{\partial E}{\partial b_k} \end{aligned} \quad (5)$$

More details regarding the NN training can be found elsewhere.¹³

3 EXPERIMENTAL AND NUMERICAL PROCEDURES

Ce-based solutions were prepared from cerium nitrate precursors ($\text{Ce}(\text{NO}_3)_3 \cdot 6\text{H}_2\text{O}$). The powder precursors were first dissolved in glacial acetic acid, which is used as a chelating agent. Eleven different amounts of Ce precursor, including (0.0499, 0.1990, 0.3490, 0.7500, 1.4900, 2.9900, 4.2500, 4.9900, 5.9900, 7.0080, 43.4000) g, which are called as concentration indexes, were used to estimate the effects on the crack formation and propagation of the coatings in the solutions as a processing parameter. The obtained solutions were subsequently diluted with isopropanol. All the solutions were stirred at room temperature for 60–120 min in order to yield transparent solutions. The thickness of the CeO_2 thin films measured by ESEM varied between 0.4 μm and 7 μm , depending on the Ce concentration in the solution. More details regarding the preparations of Ni tape and CeO_2 thin films were given in^{11,14,15}.

In order to investigate the surface morphology, the crack formation and the propagation of CeO_2 films, in-situ hot stage ESEM was used. For this procedure, Ni tape substrates were separately dipped into the eleven different Ce-based solutions at room temperature in air. Ce-based gel coatings were obtained from this process. These gel coatings were then placed in the hot-stage ESEM. The gel coatings were examined in the temperature range 24 °C to 700 °C for 5 min in vacuum conditions. After placing the Ce-based gel coatings contain-

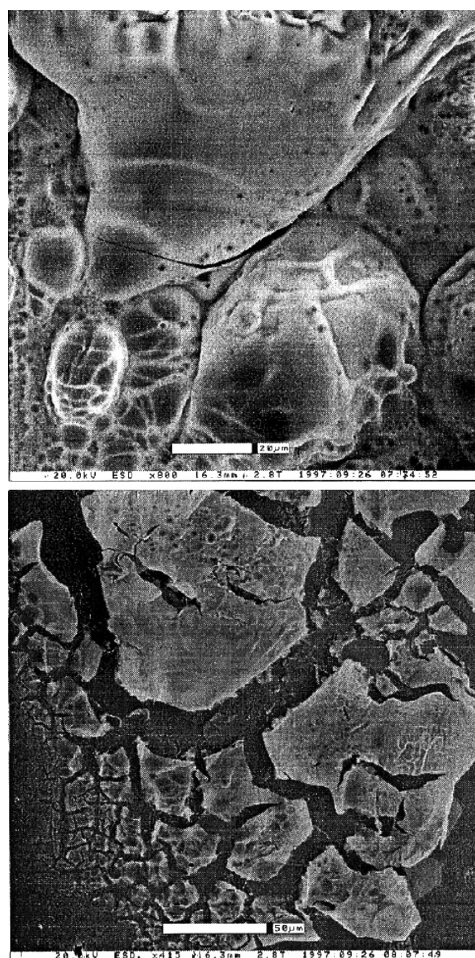


Figure 4: ESEM microstructures of Ce-based gel and CeO_2 coatings on Ni tape at: a) 25 °C and b) 600 °C¹¹

Slika 4: ESEM-posnetka koloida na osnovi premaza Ce in CeO_2 na traku iz Ni pri: a) 25 °C in b) 600 °C¹¹

ing a bubble structure in the ESEM, they were dried and heat treated from room temperature to 700 °C. The crack length and the size of the coatings were measured in the ESEM at several temperatures, i.e., (25, 100, 200, 300, 500, 600 and 700) °C, for a period of 5 min under vacuum conditions. However, here we utilized the temperatures 400 °C and 700 °C. A computer program of an in-situ hot-stage ESEM was used to measure the crack

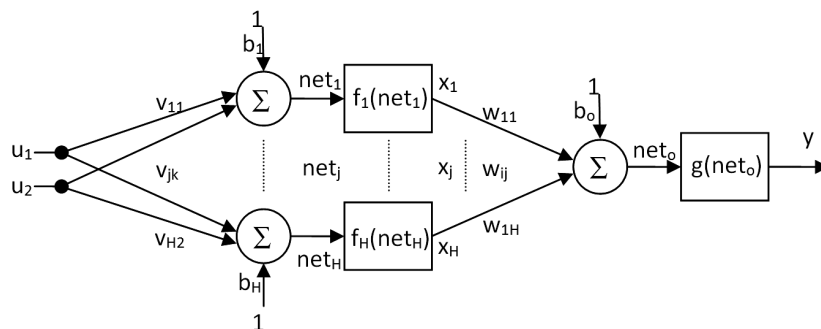


Figure 3: The used NN structure

Slika 3: Uporabljena NN-struktura

size of the coating as a function of concentration index (Ce content in the solutions) and processing temperature. In as much as the coating is a gel-like structure at 25–100 °C, and amorphous at 100–350 °C, the CeO₂ coating was formed on Ni tape at 420 °C and densified at 700 °C. For these reasons, the crack size of the CeO₂ coatings was also measured at 400 °C and 700 °C in detail. When measuring the crack sizes of the gel and oxide coatings, ESEM micrographs were taken with the scale bar 20 µm.

The NN used in this study is shown in **Figure 3**. Where v and w represent the weights, and b represents the biases. The NN has two inputs (u_1, u_2) and 1 output (y). There are six neurons in the hidden layer. $f(\cdot)$ and $g(\cdot)$ are the hidden-layer and the output-layer activation functions, respectively. The sigmoid-type activation functions are used by both layers. All the programs for the NN were developed under Matlab. The inputs of the NN represent the amount of material and the processing temperature at which the experiment was performed. The output of the NN represents the crack sizes of the coatings. The training data set contains 66 elements, includ-

Table 1: NN estimated and experimental crack sizes for 400 °C

Tabela 1: Določen NN in eksperimentalna velikost razpok pri 400 °C

Concentration index	NN inputs		NN output	
	Amount of precursor material (g)	Temperature (°C)	NN estimated crack size (µm)	Experimental crack size (µm)
1	0.0499	400	1.6309	2.4133
2	0.1990	400	1.6980	2.4345
3	0.3490	400	1.9820	2.5000
4	0.7500	400	10.2419	9.7605
5	1.4900	400	14.5338	15.0000
6	2.9900	400	14.8854	15.6250
7	4.2500	400	15.2480	17.6410
8	4.9900	400	15.6821	15.7140
9	5.9900	400	18.7295	25.0500
10	7.0080	400	9.6382	16.8900
11	43.4000	400	33.5412	30.5000

Table 2: NN estimated and experimental crack sizes for 700 °C

Tabela 2: Določen NN in eksperimentalna velikost razpok pri 700 °C

Concentration index	NN inputs		NN output	
	Amount of precursor material (g)	Temperature (°C)	NN estimated crack size (µm)	Experimental crack size (µm)
1	0.0499	700	2.2660	2.6886
2	0.1990	700	2.8976	2.6547
3	0.3490	700	5.4302	3.0000
4	0.7500	700	17.2949	13.8090
5	1.4900	700	18.5257	15.6000
6	2.9900	700	22.9032	17.5000
7	4.2500	700	55.6694	26.4710
8	4.9900	700	71.0257	44.4700
9	5.9900	700	75.8715	71.4200
10	7.0080	700	110.6222	73.9000
11	43.4000	700	142.2619	140.0000

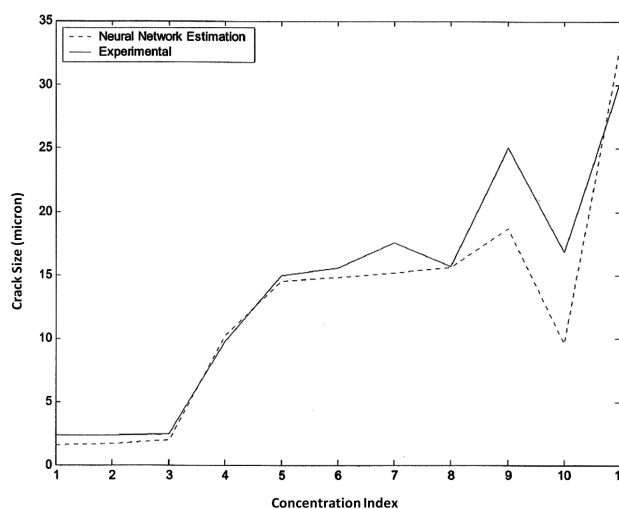


Figure 5: The NN estimation and experimental results for CeO₂ coatings on Ni tape at 400 °C. In this figure, the x and y axes indicate the crack size of the coating and the concentration index, respectively.

Slika 5: Določanje NN in rezultati preizkusov za premaz CeO₂ na traku iz Ni pri 400 °C. Na sliki x - in y -os pomenita velikost razpoke in indeks pogostosti.

ing the data for temperatures (25, 100, 200, 300, 500 and 600) °C. We left the data for temperatures 400 °C and 700 °C as the testing data sets. Both test sets contain 11 elements. A batch-training procedure was applied to train the NN using the Steepest Descent (SD) method and then the crack size of the CeO₂ buffer layer was estimated for 400 °C and 700 °C. The details of test data sets and the NN estimation results are shown in **Tables 1** and **2**.

4 RESULTS AND DISCUSSION

In-situ, hot-stage ESEM, depending on the temperature, the crack formation and propagation of the coatings were evaluated as a function of the Ce content in the solutions. **Figure 4** shows ESEM microstructures of the Ce-based gel and CeO₂ coatings on Ni tape at 25 °C and 600 °C, respectively.¹¹ The ESEM observations revealed that the crack surface of the Ce-based films changed slightly with increasing temperatures, from 25 °C to 500 °C, when compared with the other thin films. After CeO₂ formation at about 420 °C, microcracks were observed on the surface. It is interesting to note here that the bubbles and micro-bubbles were produced on the surface once the precursor material increased in this solution. The bubbles showed characteristic properties that caused the cracks to start on the surfaces of the gel films of the nitrate-salt-based precursors. Note that there are many factors influencing the bubbling problem, such as types of precursors, solvent and chelating agent, viscosity, dilution, Ce content in solution and so on. It was found that the size and propagation rate of the cracks increased with the increasing Ce content. It is clear from the ESEM observations that the measured values of the

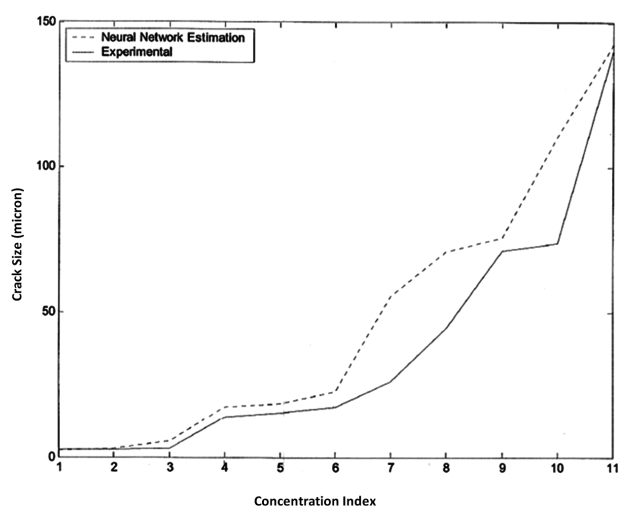


Figure 6: The NN estimation and experimental results for CeO_2 coatings on Ni tape at 700 °C. In this figure, the x and y axes indicate the crack size of the coating and the concentration index, respectively.

Slika 6: Določanje NN in rezultati preizkusov za premaz CeO_2 na traku iz Ni pri 700 °C. Na sliki x - in y -os pomenita velikost razpoke in indeks pogostosti.

crack-propagation rate altered slightly at (300, 400 and 500) °C, whereas at 600 °C they changed considerably.

Figure 5 shows the NN estimation and the experimental results for CeO_2 on Ni tape at 400 °C. In this figure, the x and y axes indicate the crack size of the coating and the concentration index, respectively. The concentration index corresponds to eleven type solutions, including several $\text{Ce}(\text{NO}_3)_3 \cdot 6\text{H}_2\text{O}$ contents. As mentioned just previously, the $\text{Ce}(\text{NO}_3)_3 \cdot 6\text{H}_2\text{O}$ precursors were dissolved using a solvent and a chelating agent. The eleven solutions were prepared by changing the amount of precursors and thus eleven type coatings were obtained using the hot-stage ESEM. As a result of this, the crack sizes were measured at 400 °C in the ESEM and the concentration index was taken as numerical values, such as from 1 to 11. Actually, the concentration indexes are not real values indicating the amount of precursor. It is clear from **Figure 5** that the estimated crack size of the coating is close to the experimental results for 400 °C. Similarly, the NN estimation and the experimental results of the crack size for 700 °C are presented in **Figure 6**. It is worth noting that the predicted result approaches the mean values when the standard deviation associated with the measurements is small. Now that the goal is to fabricate low-cost, high-quality products in a short time in a modern industry, the optimization of the processing temperature can be estimated using the NN technique. The key feature of this research is that the NN approach is useful for the prediction of the cracks size and the crack-propagation rate during the heat treatment of the sol-gel coatings. This study can be extended by using other buffer layers, depending on the sol-gel parameters. This technique is quite likely to be a key area for the development of all sol-gel films in the future, prior to the coating processes.

5 CONCLUSIONS

In summary, the NN-based approach was developed to estimate the crack sizes of a CeO_2 coating on a Ni tape for YBCO-coated conductors, depending on processing temperatures such as 400 °C and 700 °C using a hot-stage ESEM. A multilayer feed-forward NN was trained to estimate the crack size of the coating during processing at temperature in the range 24–700 °C. The experimental measurements of the crack size on the coating on the Ni tape substrate are a very expensive and a time-consuming process. The approach proposed in the present study provides simplicity and is cost-effective for preparing the new solutions and subsequent processing in the sol-gel technique.

Acknowledgements

The authors would like to thank Dr. Y. S. Hascicek and R. E. Goddard for their assistance in obtaining the ESEM micrographs at the National High Magnetic Field Laboratory of Florida State University in Tallahassee, Florida USA.

6 REFERENCES

- K. Hornik, M. Stinchcombe, H. White, *Neural Networks*, 2 (1989), 359–366
- K. J. Hunt, D. Sbarbaro, R. Zbikowski, P. J. Gawthrop, *Automatica*, 28 (1992), 1083–1112
- M. Agarwal, *IEEE Control Systems Magazine*, 17 (1997), 75–93
- K. S. Narendra, K. Parthasarathy, *IEEE Transactions on Neural Networks*, 1 (1990), 4–27
- A. G. Parlos, S. K. Menon, A. F. Atiya, *IEEE Transactions on Neural Networks*, 12 (2001), 1411–1432
- I. H. Mutlu, E. Celik, M. K. Ramazanoglu, Y. Akin, Y. S. Hascicek, *IEEE Transactions on Applied Superconductivity*, 10 (2000), 1154–1157
- E. Celik, I. H. Mutlu, Y. S. Hascicek, *IEEE Transactions on Applied Superconductivity*, 10 (2000), 1162–1166
- E. Celik, H. Okuyucu, I. H. Mutlu, M. Tomsic, J. Schwartz, Y. S. Hascicek, *IEEE Transactions on Applied Superconductivity*, 11 (2001), 3162–3165
- H. Okuyucu, E. Celik, M. K. Ramazanoglu, Y. Akin, I. H. Mutlu, W. Sigmund, J. E. Crow, Y. S. Hascicek, *IEEE Transactions on Applied Superconductivity*, 11 (2001), 2889–2892
- X. D. Wu, S. R. Foltyn, P. Arendt, J. Townsend, I. H. Campbell, P. Tiwari, Q. X. Jia, J. O. Willis, M. P. Maley, J. Y. Coulter, D. E. Peterson, *IEEE Transactions on Applied Superconductivity*, 5 (1995), 2001–2006
- E. Celik, Y. S. Hascicek, *Materials Science & Engineering B*, 94 (2002), 176–180
- P. J. Werbos, *Beyond Regression, New Tools for Prediction and Analysis in the Behavioral Sciences*, PhD. Dissertation, Harvard University, Boston, USA, 1974
- M. S. Al-Haik, H. Garmestani, A. Savran, *International Journal of Plasticity*, 20 (2004), 1875–1907
- E. Celik, J. Schwartz, E. Avci, H. J. Schneider-Muntau, Y. S. Hascicek, *IEEE Transactions on Applied Superconductivity*, 9 (1999), 2264–2268
- E. Celik, H. I. Mutlu, E. Avci, Y. S. Hascicek, *Advances in Cryogenic Engineering (Materials)*, 46 (1999), 895–900